Protoplasma 124, 1—9 (1985)

PROTOPLASMA

Cytochemical and X-Ray Microanalysis Studies of Intracellular Calcium Pools in Scale-Bearing Cells of the Coccolithophorid *Emiliania huxleyi*

P. VAN DER WAL[1,*], W. C. DE BRUIJN[2], and P. WESTBROEK[1]

[1] Department of Biochemistry, University of Leiden
[2] Centre for Analytical Electron Microscopy, Laboratory for Electron Microscopy, University of Leiden

Received March 8, 1984
Accepted in revised form April 25, 1984

Summary

Emiliania huxleyi is a coccolithophorid with a life cycle including a stage characterized by the occurrence of a scale-bearing cell type. The scales are composed of organic material and are produced in the cisternae of the Golgi apparatus. The present report deals with the ultrastructural calcium localization in scale-bearing cells using cation-precipitating agents. Cations were precipitated either with potassium pyroantimonate alone or according to a combined procedure in which cells are treated first with potassium oxalate, or potassium carbonate, or potassium phosphate, and then with potassium pyroantimonate. The distribution of electron-opaque deposits was the same when visualized by all four techniques. The most extensive deposits occurred in the Golgi apparatus, the "peripheral space" (a cellular compartment totally encompassing the protoplast), the multivesicular bodies, and the cell vacuole. X-ray microanalysis revealed that calcium was a constituent of the electron-opaque deposits. The uptake and transport of calcium, as universal functions of the Golgi apparatus, are discussed.

Keywords: Calcium localization; Coccolithophorids; *Emiliania huxleyi;* Pyroantimonate; Ultrastructure; X-ray microanalysis.

1. Introduction

Emiliania huxleyi Hay and Mohler is a planktonic, unicellular alga (*Prymnesiophyceae*) (HIBBERD 1976, PARKE and GREEN 1976). It belongs to the group of coccolith-bearing protoctists and is one of the commonest species in the marine environment. At least two cell types form part of its regular life cycle, viz., scale-bearing cells (S cells) and coccolith-bearing cells (C cells) (KLAVENESS 1972 b). S cells possess two flagella and are covered with one or several layers composed of what are called scales. The scales are formed in the cisternae of the Golgi apparatus. C cells do not possess flagella or scales; in a specialized organelle, possibly derived from the Golgi apparatus (KLAVENESS 1972 a, VAN DER WAL *et al.* 1983 b), they produce calcified structures called coccoliths. Once formed, the coccoliths are extruded and incorporated into the "coccosphere", *i.e.,* a covering formed of one or several layers of coccoliths surrounding the cell.

S cells lack the specific intracellular system required to produce coccoliths, but mineralization does occur in these cells: crystals of unknown nature, embedded in a densely staining matrix, have been observed within a single large vacuole, called body-X (WILBUR and WATABE 1963). Beneath the coccoliths or scales the cell of *E. huxleyi* is surrounded by a distinct "membranous cover" (KLAVENESS 1972 a, b).

The subcellular distribution of calcium in the S cells was investigated using potassium pyroantimonate as a precipitating agent. Also, a combined potassium oxalate-potassium pyroantimonate precipitating technique was employed, Ca^{2+} being expected to be precipitated as the sole cation (BORGERS *et al.* 1977, 1981, SHAW and MORRIS 1980). Besides K-oxalate, use was made of K-phosphate and K-carbonate as the primary cation-precipitating agents, in an attempt to localize different kinds of calcium pools (M. BORGERS, pers. comm.).

* Correspondence and Reprints: Department of Biochemistry, University of Leiden, Wassenaarseweg 64, 2333 AL Leiden, The Netherlands.

2. Material and Methods

2.1. Cell Strain and Culture Conditions

The study was done in scale-bearing cells originating from the calcifying strain A 92, parent cells of which were kindly put at our disposal by Dr. GUILLARD of Woods Hole Oceanographic Institution (U.S.A.). In our laboratory some cultures of this strain spontaneously altered into cultures containing only scale-bearing cells.
Cells were grown at 18 °C in 500 ml Erlenmeyer flasks containing 100 ml enriched sea-water medium (Eppley's medium, see DE JONG 1975). The cultures were exposed to a continuous cycle of 16 hours of light and 8 hours of darkness. In all experiments only actively growing cells were used.

2.2. Cation Localization

2.2.1. Precipitation of Calcium by Pyroantimonate Alone

Cells were fixed for 16 hours at 4 °C in a solution containing 3% glutaraldehyde, 2% (~ 80 mM) pyroantimonate, and 0.4 M sucrose. The fixative was brought to pH 7.4 with potassium hydroxide (KOH), after which the cells were rinsed by immersion first for 45 minutes at 4 °C in a solution of 2% pyroantimonate with 0.4 M sucrose and then in a solution of 2% pyroantimonate containing 0.2 M sucrose for 30 minutes at the same temperature. The pH of the washing solutions was adjusted to 7.4 with KOH. The cells were then postfixed for 3 hours at 4 °C in a solution containing 1% OsO_4 and 2% K-pyroantimonate. The fixative was prepared as follows: 4 g K-pyroantimonate (Merck) was added to 100 ml 0.01 N acetic acid brought to pH 7.6 with KOH, the K-pyroantimonate being dissolved by heating the mixture without allowing it to boil; then, equal amounts of this solution, cooled to room temperature, and of a solution containing 2% OsO_4, were mixed, and the fixative was brought to pH 7.4 with KOH. After postfixation, the cells were rinsed for 15 minutes at 4 °C in distilled water brought to pH 10 with KOH. Further handling of the cells is described below.

2.2.2. Precipitation of Calcium with Combined Methods

Cells were fixed for 2–4 hours in a solution containing 3% glutaraldehyde, 90 mM potassium oxalate, and sufficient sucrose to approximate the tonicity of the growth medium. The fixative was brought to pH 7.4 with potassium hydroxide (KOH), after which the cells were rinsed by immersion first for 1.5 hours at 4 °C in a solution of 90 mM K-oxalate with 0.4 M sucrose and then in a solution of 90 mM K-oxalate containing 0.2 M sucrose for 17 hours at the same temperature. The pH of the washing solutions was adjusted to 7.4 with KOH. The cells were then postfixed for 2 hours at 4 °C in a solution containing 1% OsO_4 and 2% potassium pyroantimonate. The fixative was prepared as described above. After postfixation, the cells were rinsed for 45 minutes at 4 °C in 2% K-pyroantimonate, the pH of which had been adjusted to 7.4 with KOH, and then given a second rinse for 15 minutes in distilled water brought to pH 10 with KOH.
We also used phosphate-pyroantimonate and carbonate-pyroantimonate precipitating techniques differing from the above procedure in that the oxalate in the glutaraldehyde fixative and the washing solutions was replaced by 90 mM potassium phosphate and potassium carbonate, respectively. Another difference was that the pH of the carbonate-containing solutions was brought to 8. The cation-precipitating techniques we employed are a modification of the combined oxalate-pyroantimonate technique introduced by BORGERS *et al.* (1977).

After the final wash, the cells were embedded in 2% agar and dehydrated in a graded series of ethanol, after which the blocks of agar containing the cells were embedded in Epon. Ultrathin sections, cut on a LKB ultramicrotome, were viewed in a Philips EM 200 or 400 electron microscope either without poststaining, or after double staining with lead hydroxide and uranyl acetate.
X-ray microanalysis of cell constituents was performed in unstained ultrathin sections.

2.3. X-Ray Microanalysis

X-ray microanalysis was performed in ultrathin sections of specimens prepared according to one of the four precipitating techniques described above using an analytical electron microscope (Philips EM 400) equipped with a Tracor/Northern energy-dispersive X-ray analyser and connected to a computer. The computer was programmed with the standard software packages. Grids with the ultrathin sections were mounted in a low-background holder and tilted 24° toward the X-ray detector. Static point analyses were performed in the CTEM mode with beam diameters of 100, 200, and 400 nm at 80 kV. The instrument was fitted with spray apertures to minimize X-ray excitation. Spectra were recorded in the range of either 0.5–5.0 keV or 0.5–20.0 keV.
The main purpose of the X-ray microanalysis studies was to determine whether each of the four cation-precipitating techniques employed led to specific precipitation of Ca^{2+} ions. A serious problem encountered was that the major X-ray spectral lines of calcium, viz., $Ca_{K\alpha}$ at 3.695 keV and $Ca_{K\beta}$ at 4.012 keV, are considerably overlapped by the spectral lines of the L series of antimony ($Sb_{L\alpha}$ at 3.604 keV, $Sb_{L\beta 1}$ at 3.843 keV, and $Sb_{L\beta 2}$ at 4.100 keV). We attempted to determine the presence or absence of calcium in the pyroantimonate deposits unambiguously by subtracting a standard spectrum, obtained by analysis of a calcium-free antimony salt, from the tissue spectrum as follows. As standard we used ultrathin sections of potassium pyroantimonate powder embedded in Epon, an X-ray spectrum of which was recorded and stored on tape. In this standard spectrum the intensity of the $Sb_{L\alpha}$ in the range of 3,600–3,640 eV amounted to 1,020 counts and the intensity of the $Sb_{L\beta 1}$ in the range of 3,840–3,880 eV to 627 counts. Recording of X-ray spectra of pyroantimonate deposits in the cells was stopped when the intensity in the channel of 3,840–3,880 eV reached a value of 627 counts, which is the height of the $Sb_{L\beta 1}$ peak in the same channel in the standard spectrum. Next, the computer was used to substract the standard spectrum from the tissue spectrum. The identification of the resultant peaks was done automatically by the IDENT program. Normalization of the tissue spectrum and standard spectrum was sometimes performed at the $Sb_{L\alpha}$ spectral line, as had also been done by VAN IREN *et al.* (1979) and BURGER and DE BRUIJN (1979), but usually at the $Sb_{L\beta 1}$ spectral line, because this line is less affected by the presence of potassium ($K_{K\alpha}$ at 3,312 eV and $K_{K\beta}$ at 3,589 eV) and calcium than the $Sb_{L\alpha}$ spectral line.

3. Results

3.1. Ultrastructural Distribution of Precipitates

The cation-precipitating techniques used in this study had a destructive effect on most of the cells, but the cells which could be analysed showed a microanatomy comparable to that encountered in cells double fixed in glutaraldehyde and OsO_4 (*cf.*, KLAVENESS 1972 a, b, WILBUR and WATABE 1963). These non-distorted cells

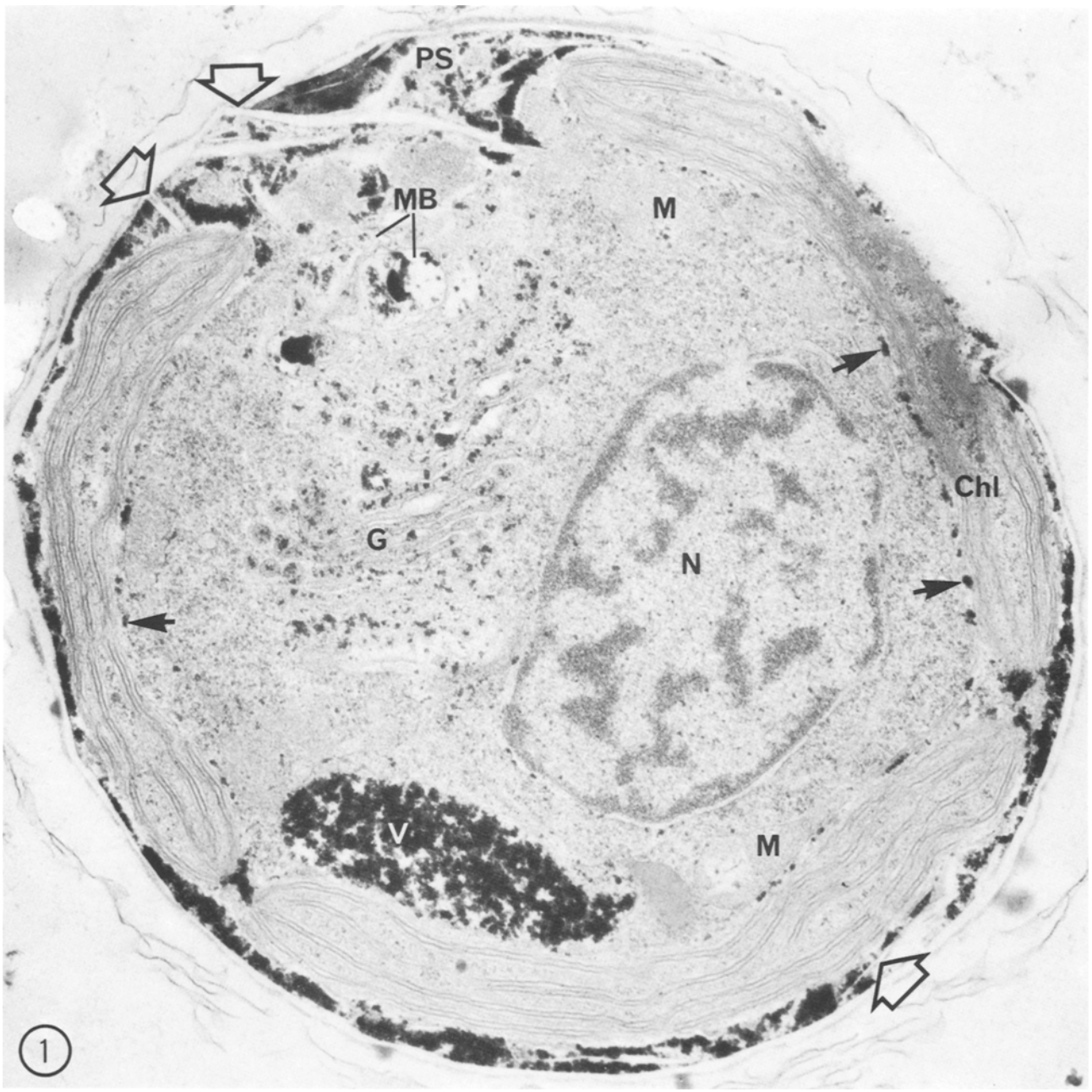

Fig. 1. Micrograph of ultrathin section of S cell treated according to the combined phosphate/pyroantimonate cation-precipitating method. Extensive electron-opaque deposits occur in the peripheral space (*PS*), cell vacuole (*V*), Golgi apparatus (*G*), and multivesicular bodies (*MB*), as well as at the tips of chloroplasts (*Chl*). Large grains of precipitate occur in the plastidal envelope (arrows). Also indicated are mitochondria (*M*). Note the electron-translucent bands occurring in the peripheral space (open arrows). Prefixed in glutaraldehyde + potassium phosphate, postfixed in OsO_4 + potassium pyroantimonate. The ultrathin section was stained with uranyl acetate and lead hydroxide. × 44,000

showed electron-dense deposits with a well-defined localization, whereas the distorted cells lacked precipitates or the amount of deposit was greatly reduced. An important finding is that the use of the pyroantimonate method and the combined oxalate-, phosphate-, and carbonate-pyroantimonate methods (Figs. 1, 2, and 3) did not lead to any differences in the distribution of dense precipitates. The description that follows therefore applies to all four experiments.

The highest concentrations of precipitate were found at four subcellular sites (*cf.*, Fig. 1): 1. Golgi apparatus, 2. "cell vacuole", 3. multivesicular bodies, and 4. "peripheral space". With respect to these sites, the following may be said:

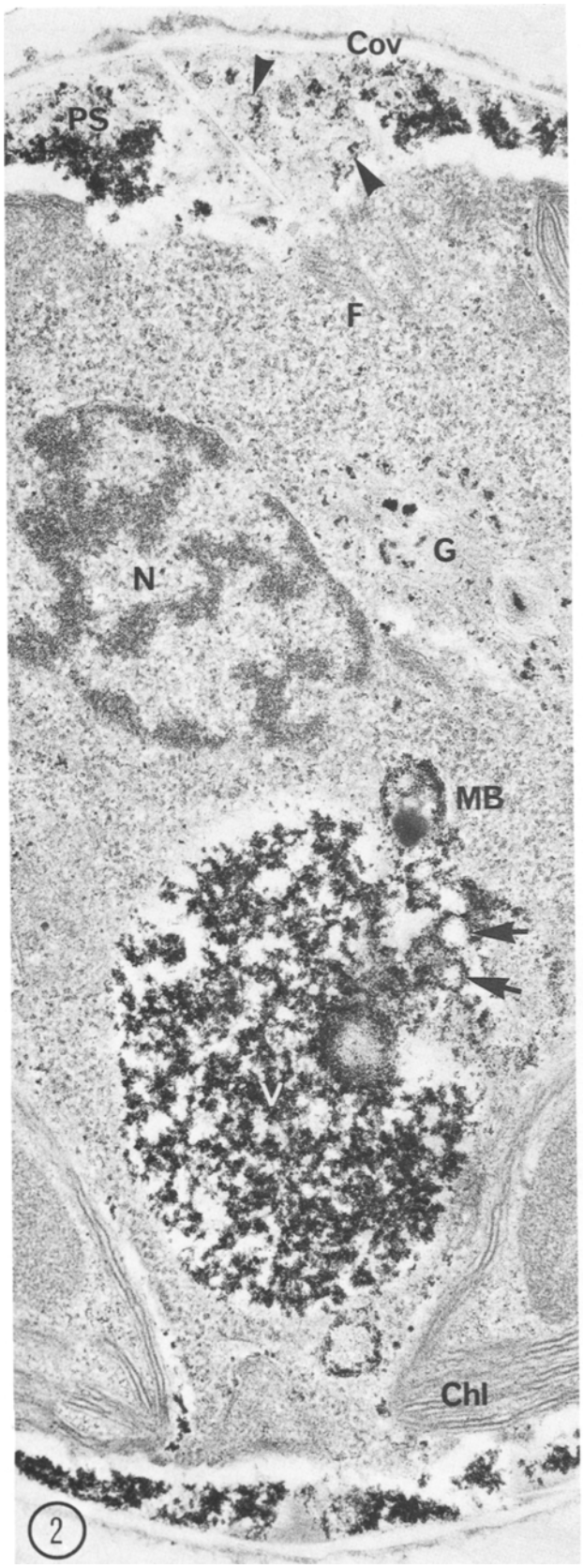

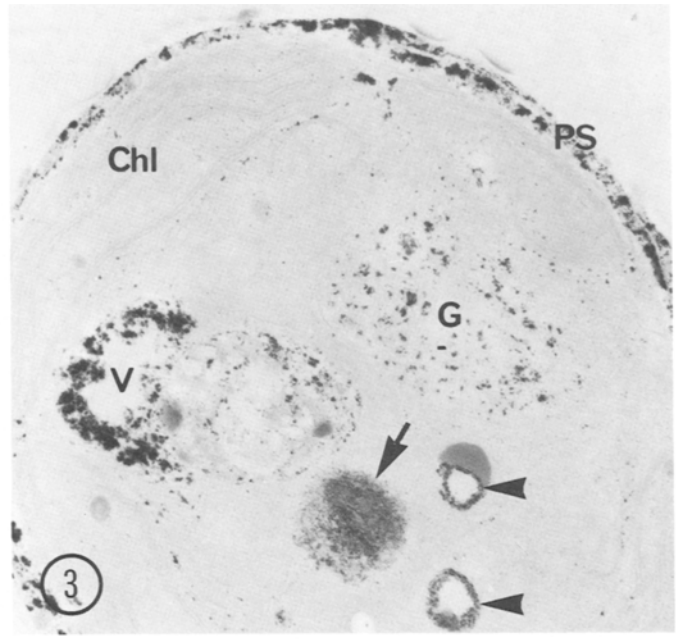

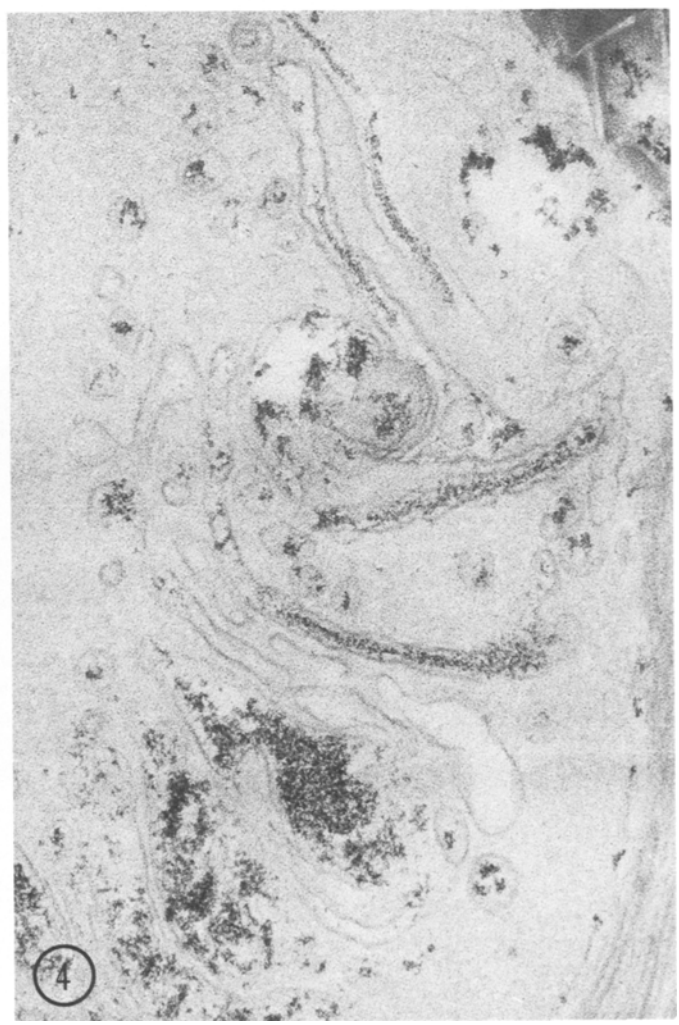

Figs. 2–4

1. Vesicles and cisternae containing electron-dense deposits in the lumen occur throughout the Golgi apparatus, but there are also some which are devoid of any precipitate in the plane of the section (Fig. 4). Pyroantimonate was probably precipitated on scales in the four distalmost cisternae in Fig. 4, as judged from the linear deposits.

2. Cells of *E. huxleyi* possess a "cell vacuole", a large organelle positioned near the periphery of the cell and clenched between plastids. In S cells it may contain birefringent particles, in which case it is called a body-X, a term introduced by WILBUR and WATABE (1963). Birefringent matter was not found in the cell vacuole after treatment of the cells with the cation-precipitating agents. Usually, the precipitate fills the entire lumen of the cell vacuole. In some cases the contours of rounded bodies are discernible (Fig. 2, arrows).

3. Multivesicular bodies lie close to the Golgi apparatus (Fig. 1) and the cell vacuole (Fig. 2). Pyroantimonate deposits occur in and outside the vesicles contained within the multivesicular bodies. The vesicles are comparable in size and morphology to the rounded bodies encountered in the cell vacuole, and for convenience they too will be called rounded bodies.

4. The peripheral space is a cellular compartment situated between the cytoplasmic margin and the membranous cell cover (Fig. 2, *Cov*). As will be shown in a detailed report on the membranous layers enveloping the cell of *E. huxleyi*, which is in preparation, both the proximal boundary of the peripheral space and the distal boundary of the cell cover are biomembranes. The peripheral space may contain rounded bodies comparable in size and morphology to those encountered in the cell vacuole and the multivesicular bodies (Fig. 2). The peripheral space often shows electron-translucent bands bounded on each side by a thin, smooth, electron-dense layer sometimes seen to be continuous with the outer boundary of the peripheral space (Fig. 1, open arrows). Analysis of serial sections showed that these layers lie roughly in parallel. Pyroantimonate precipitates in the peripheral space may occur outside and within the rounded bodies (Fig. 2).

High concentrations of deposit are often found at the tips of the chloroplasts (Fig. 1) and the peripheral parts of both lipid droplets and vacuoles with otherwise electron-translucent contents (Fig. 3). Coarse grains of pyroantimonate deposit are often dispersed in the plastidal envelope (Fig. 1, arrows), *i.e.*, a cisterna that completely surrounds the chloroplast and that has open connections with the endoplasmic reticulum. A similar precipitate is sometimes found in the lumen between the inner and the outer membranes of mitochondria (not shown).

Low concentrations of a fine-grained deposit may be found in the nuclear envelope, the heterochromatinic part of the nucleus, the endoplasmic reticulum, the cytoplasmic ground-substance, the mitochondria, and the stroma of the chloroplasts.

3.2. X-Ray Microanalysis

All deposits present at the subcellular sites mentioned in the foregoing section were shown by X-ray microanalysis to contain antimony. The major X-ray spectral lines of calcium are considerably overlapped by the spectral lines of the L series of antimony. To find out whether a calcium signal was hidden under the latter, a standard spectrum obtained from a calcium-free antimony salt was subtracted from the tissue spectrum normalized to the standard spectrum (see under Material and Methods). The standard spectrum used is shown in Fig. 5 where, to further illustrate the procedure employed, a normalized tissue spectrum and the spectrum resulting from subtraction are also shown.

Fig. 2. Micrograph of ultrathin section of S cell treated according to the combined oxalate/pyroantimonate cation-precipitating method. Rounded bodies are shown to occur in the peripheral space (*PS*) (at arrowheads), in a multivesicular body (*MB*), and in the cell vacuole (*V*) (at arrows). Also indicated are chloroplast (*Chl*), membranous cell cover (*Cov*), flagella bases (*F*), Golgi apparatus (*G*), and nucleus (*N*). Prefixed in glutaraldehyde + potassium oxalate, postfixed in OsO_4 + potassium pyroantimonate. The ultrathin section was stained with uranyl acetate and lead hydroxide. × 54,000

Fig. 3. Micrograph of ultrathin section of S cell treated according to the combined carbonate/pyroantimonate cation-precipitating method. Note that extensive electron-opaque deposits are associated with what is probably a lipid droplet (arrow) and with the peripheral parts of vesicles having otherwise electron-translucent contents (arrowheads). Also indicated are chloroplast (*Chl*), peripheral space (*PS*), cell vacuole (*V*), and Golgi apparatus (*G*). Prefixed in glutaraldehyde + potassium carbonate, postfixed in OsO_4 + potassium pyroantimonate. Unstained ultrathin section. × 20,000

Fig. 4. Distal part of Golgi apparatus. Electron-opaque deposits are restricted to membrane-bound compartments. Some vesicles and cisternae are devoid of precipitate. The deposits in the four distalmost cisternae are linear and probably demarcate scales in formation. Prefixed in glutaraldehyde + potassium oxalate, postfixed in OsO_4 + potassium pyroantimonate. The ultrathin section was stained with uranyl acetate and lead hydroxide. × 92,000

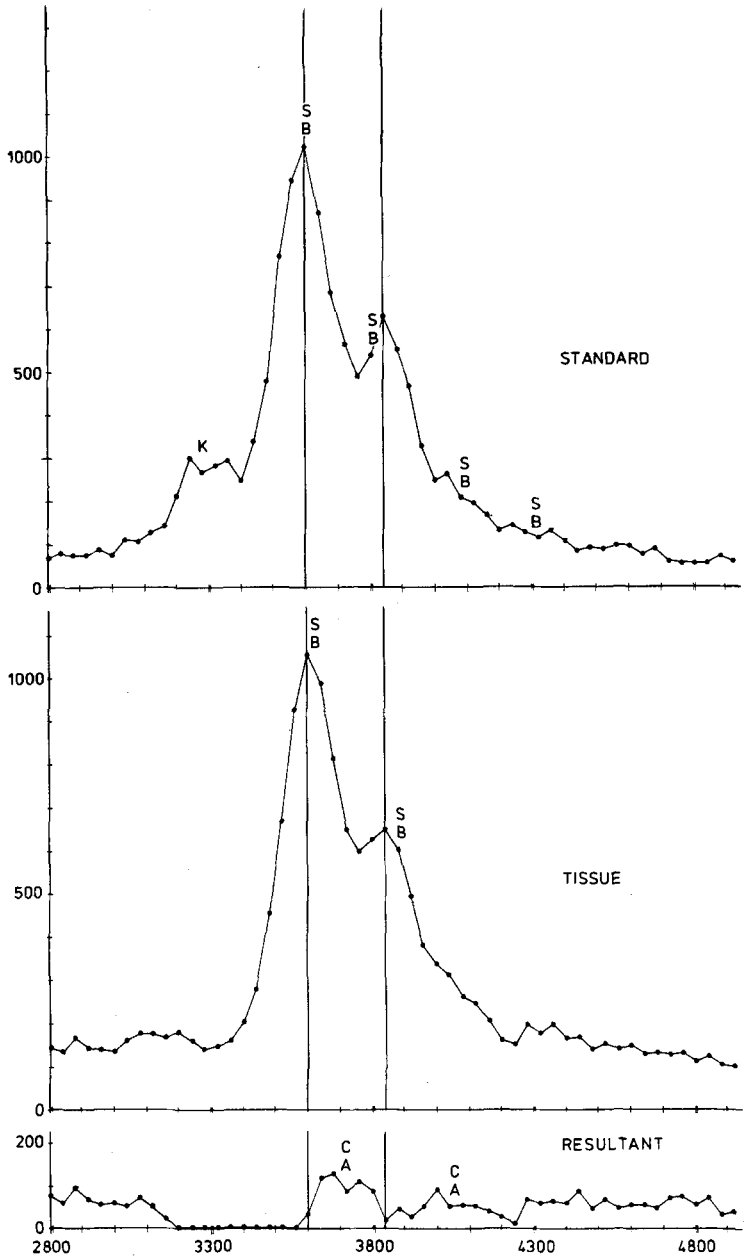

Fig. 5. Three X-ray spectra, from top to bottom: 1. Spectrum of a potassium-pyroantimonate deposit used as standard in this study; 2. spectrum of a pyroantimonate deposit obtained with the combined carbonate/pyroantimonate method in the cell vacuole of *E. huxleyi* (this spectrum was normalized at 3,840–3,880 eV to the standard spectrum shown above); 3. resultant spectrum obtained by subtraction of the standard spectrum from the tissue spectrum. The identification of the peaks was done automatically by the IDENT program. The two vertical lines in the spectra mark the position of the $Sb_{L\alpha}$ and the $Sb_{L\beta 1}$ spectral line, respectively. Vertical scale in counts per channel; horizontal scale in eV

The latter, called the resultant spectrum, clearly reveals that calcium forms a constituent part of the electron-opaque deposits. Many tens of analyses of deposits obtained with the four techniques were similarly performed and invariably showed the presence of calcium. Fig. 6 shows some of the resultant spectra obtained for electron-opaque deposits present in various cellular compartments after use of the four cation-precipitating techniques.

The intensities of the spectral lines of calcium in the resultant spectra give a measure of the ratio of calcium and antimony in the electron-opaque deposits. Tab. 1 lists for each of the precipitating methods used the mean and the standard deviation of the intensities of the $Ca_{K\alpha}$ peak in the resultant spectra obtained in this study. The Kruskal-Wallis rank test showed that these samples originated from populations that do not differ significantly at the 5% level of significance.

Table 1. *Demonstration of calcium in intracellular deposits of pyroantimonate by X-ray microanalysis*

Precipitating method	Mean ± std. dev. of intensities (counts) [1] in the range of 3,600–3,800 eV [2]	Number of analyses
Carbonate/pyroantimonate	451 ± 162	10
Oxalate/pyroantimonate	613 ± 290	11
Phosphate/pyroantimonate	486 ± 222	15
Pyroantimonate	640 ± 208	11

[1] Results obtained after subtraction of a standard potassium pyroantimonate spectrum, with the understanding that the tissue spectrum was normalized to the gross intensity of 627 counts in the spectral range 3,840–3,880 eV in the standard spectrum.
[2] Spectral area where $Ca_{K\alpha}$ emission was to be expected.

In the deposits obtained with the oxalate-pyroantimonate technique potassium was detected occasionally (Fig. 6) and sometimes sodium as well. None of the X-ray spectra of the deposits obtained with the other three precipitating techniques showed these two elements.

Normalization of a tissue spectrum to the $Sb_{L\alpha}$ spectral line in the standard spectrum was also done in a few cases. Subtraction of the standard spectrum from the tissue spectrum normalized in this way again demonstrated that a Ca-signal was hidden under the spectral lines of antimony.

Analyses of cellular parts lacking electron-dense deposits never revealed the presence of Sb, Ca, K, or Na.

4. Discussion

4.1. Cation Localization

Irrespective of the precipitating techniques employed S cells of *E. huxleyi* with a well-preserved morphology showed extensive deposits of pyroantimonate located at specific sites within membrane-bound cellular compartments. Probably, no large-scale dislocation of cations occurred in these cells during the preparative procedure, only minor displacements occurring within the compartments. Cells with a poorly preserved microanatomy showed markedly less or no precipitate, which might indicate that many or all of the cations originally present in these cells were extracted during the preparation. The cells that did not suffer from internal distortion were probably protected in some way by a favorable microenvironment and /or by favorable intracellular conditions.

X-ray microanalysis of the deposits revealed that the phosphate-pyroantimonate the carbonate-pyroantimonate, and the pyroantimonate techniques can be successfully utilized to specifically demonstrate the presence of intracellular calcium. The combined oxalate-pyroantimonate method is less specific in this respect since we have found that by using this technique potassium and sodium were precipitated as well in a number of cases.

The use of four different precipitating agents (at approximately the same molar concentration) each forming a calcium salt with a different solubility, was meant to discriminate between pools of bound calcium differing from one another in the range of solubilities of the calcium complexes they contain. We shall refer to these pools as chemical pools. The distribution patterns of the pyroantimonate deposits obtained with each of the four techniques were identical. In other words, a topographic distinction between the pools was not achieved. If the precipitating techniques are indeed discriminative, this might indicate that chemical pools of bound calcium completely overlap each other in the S cells of *E. huxleyi.*

Outside the pyroantimonate deposits obtained with the four precipitating techniques, no Ca^{2+} or other cations could be detected by X-ray microanalysis. Thus, calcium at these sites is either absent or, if present, occurs in amounts below the detection limit of the analytical electron microscope ($\sim 0.5\%$).

The peripheral space, the cell vacuole, and the multivesicular bodies are among the cellular sites with the highest concentration of calcium and all three contain rounded bodies. This resemblance in contents suggests that these compartments are functionally related.

4.2. Calcium Sequestration by the Golgi Apparatus

The extensive pyroantimonate deposits observed in the Golgi apparatus strongly suggest that the sequestration of Ca^{2+} ions is an important function of this organelle. In algae that produce so-called heterococcoliths (TAPPAN 1980), like the C cells of *E. huxleyi,* this function of the Golgi apparatus is readily demonstrated, since these coccoliths, in which large amounts of calcium accumulate, are produced within this compartment or in a Golgi-derived organelle. As shown by VAN DER WAL *et al.* (1983 a), the Golgi apparatus in *Hymenomonas carterae* contains a second pool of Ca^{2+} in the form of granular bodies called coccolithosomes. Both the coccolithosomes and the coccoliths of this species were found to be associated with polysaccharides. Polysaccharides were found to form an integral part of the coccoliths of *E. huxleyi* too (VAN DER WAL *et al.* 1983 b) and a Ca^{2+}-binding polysaccharide

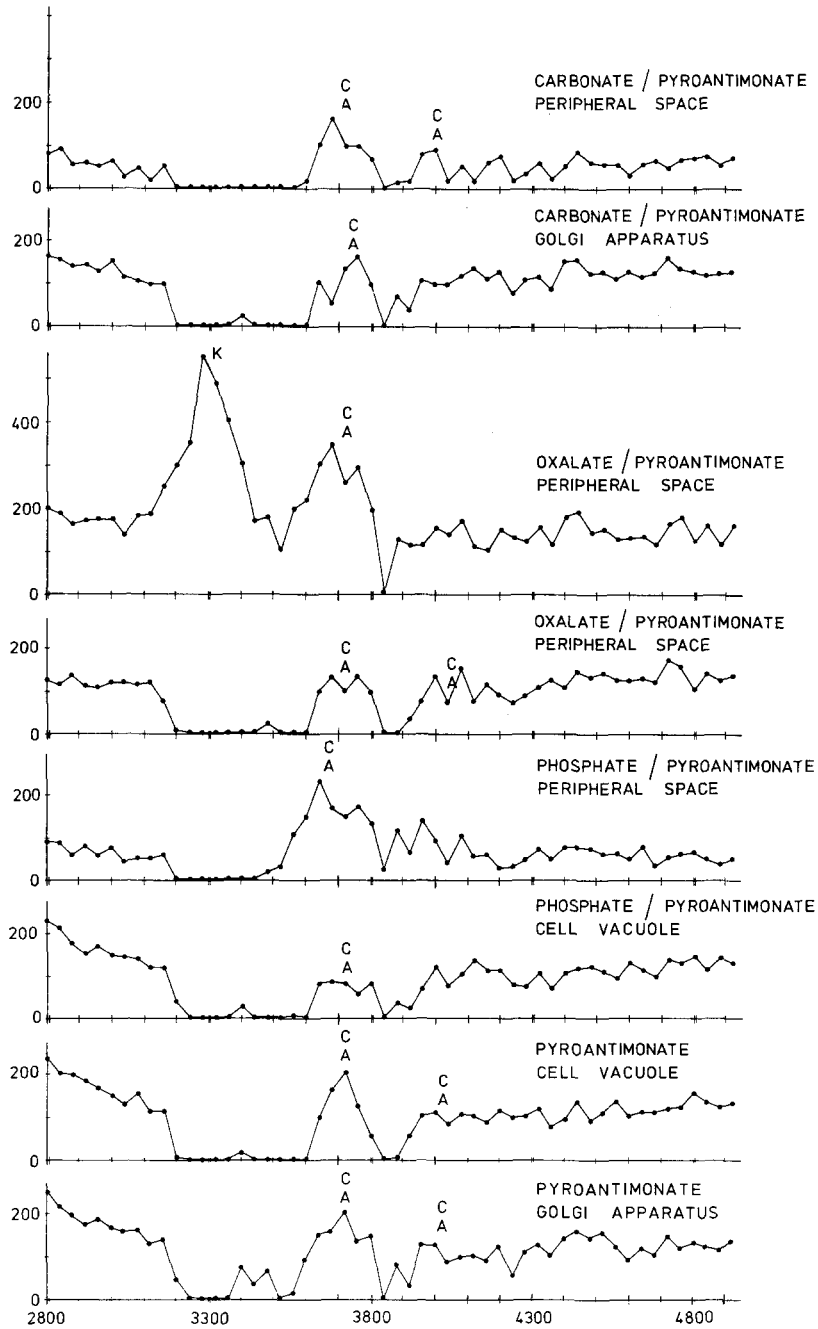

Fig. 6. X-ray spectra resulting from the subtraction of a standard spectrum of potassium pyroantimonate from spectra normalized to it at 3,840–3,880 eV, obtained from pyroantimonate deposits formed at some well-defined sites in the cell with the four precipitating methods employed. The identification of the peaks was done automatically by the IDENT program. One peak in these spectra was always identified as the $Ca_{K\alpha}$ peak; in some spectra the $Ca_{K\beta}$ peak was identified as well. Vertical scale in counts per channel; horizontal scale in eV

has been isolated from these particles (DE JONG *et al.* 1976, 1979). It was hypothesized that constituent carboxyl and sulphate groups are responsible for the Ca^{2+}-binding capacity of this compound. Possibly, Ca^{2+} sequestration by the Golgi apparatus of S cells is also performed by binding of Ca^{2+} to acid polysaccharides. If so, this phenomenon might ultimately by the result of the capacity of the Golgi apparatus to carboxylate and /or to sulphate polysaccharides. Coccolithophorids are not unique in having a Golgi apparatus capable of sequestering Ca^{2+}. In many invertebrates intracellular calcification seems to be performed in Golgi-derived vesicles (*cf.*, WATABE and WILBUR 1976). Furthermore, in a number of animal cells pyroantimonate-mediated Ca^{2+} precipitates have been found in close association with the vesicles and the

cisternae of the Golgi apparatus (for references, see WICK and HEPLER 1982). In addition, FREEDMAN *et al.* (1977) concluded from *in vitro* experiments on rat intestinal membrane vesicles that the Golgi apparatus may be involved in the intracellular accumulation of Ca^{2+}. Further investigations showed this accumulation to be the result of an ATP-independent carrier-mediated transport followed by binding of Ca^{2+} to the vesicle (FREEDMAN *et al.* 1981). The Ca^{2+} influx was thought to be accomplished by a countertransport mechanism, the uptake of Ca^{2+} being linked to the release of Mg^{+}, Sr^{2+}, or H^{+}.

Ca^{2+} accumulation seems to be a universal feature of the Golgi apparatus. Possibly, the mechanism of Ca^{2+} transport associated with this organelle is universal too. If a Ca^{2+}/H^{+} countertransport mechanism exists in coccolithophorids, the production of coccoliths has a stimulatory effect on the Ca^{2+} accumulation in the vesicle in which these particles are formed, because the process of calcification releases protons. These protons can be exchanged across the vesicular membrane for the Ca^{2+} ions present in the cytoplasm. This process may continue over a considerable period if both Ca^{2+} and H^{+} are neutralized after being exchanged. On one side of the vesicular membrane Ca^{2+} is precipitated in crystalline $CaCO_3$, on the other side the decrease in pH by the extrusion of H^{+} from the calcification site may be compensated for by photosynthesis, which via CO_2 removal causes the intracellular pH to rise (*cf.*, SIKES *et al.* 1980).

Acknowledgements

We are indebted to Prof. W. TH. DAEMS, Prof. A. BROUWER, Prof. L. BOSCH, and Dr. E. W. DE VRIND-DE JONG for advice during the course of our investigations and for their critical reading of the manuscript. Thanks are also due to Dr. M. BORGERS for his valuable advices and to Dr. H. J. BLANKSMA at the Computer Centre of Leiden University for advice and for performing the non-parametric statistical test. We also wish to thank Mr. L. D. C. VERSCHRAGEN, Mr. J. J. BEENTJES, Mr. L. WELMERS, and Mr. G. VAN TOL for photographic assistance, Mrs. I. BOOGAARD for secretarial assistance, and Mrs. I. SEEGER for reading the English text.

References

BORGERS, M., BRABANDER, M. DE, REEMPTS, J. VAN, AWOUTERS, F., JACOB, W. A., 1977: Intranuclear microtubules in lung mast cells of guinea pigs in anaphylactic shock. Lab. Invest. **37**, 1—8.

— THONÉ, F., NUETEN, J. M. VAN, 1981: The subcellular distribution of calcium and the effects of calcium antagonists as evaluated with a combined oxalate-pyroantimonate technique. Acta Histochemica, Suppl.-Band **24**, 327—332.

BURGER, E. H., BRUIJN, W. C. DE, 1979: Mitochondrial calcium of intact and mechanically damaged bone and cartilage cells studied with K-pyroantimonate. Histochemistry **62**, 325—336.

FREEDMAN, R. A., WEISER, M. M., ISSELBACHER, K. J., 1977: Calcium translocation by Golgi and lateral-basal membrane vesicles from rat intestine: Decrease in vitamin D-deficient rats. Proc. Nat. Acad. Sci. **74**, 3612—3616.

— MACLAUGHLIN, J. A., WEISER, M. M., 1981: Properties of Ca^{2+} uptake and release by Golgi membrane vesicles from rat intestine. Arch. Biochim. Biophys. **206**, 233—241.

HIBBERD, D. J., 1976: The ultrastructure and taxonomy of the *Chrysophyceae* and *Prymnesiophyceae* (*Haptophyceae*): A survey with some new observations on the ultrastructure of the *Chrysophyceae*. Botanical J. Linnean Soc. **72**, 55—80.

IREN, F. VAN, ESSEN-JOOLEN, L. VAN, DUYN SCHOUTEN, P. VAN DER, BOERS-VAN DER SLUIJS, P., BRUIJN, W. C. DE, 1979: Sodium and calcium localization in cells and tissues by precipitation with antimonate: a quantitative study. Histochemistry **63**, 273—294.

JONG, E. W. DE, 1975: Isolation and characterization of polysaccharides associated with coccoliths. Ph.D. Thesis, University of Leiden, The Netherlands.

— BOSCH, L., WESTBROEK, P., 1976: Isolation and characterization of a Ca^{2+}-binding polysaccharide associated with coccoliths of *Emiliania huxleyi* (Lohmann) Hay and Mohler. Eur. J. Biochem. **70**, 611—621.

— RENS, L. VAN, WESTBROEK, P., BOSCH, L., 1979: Biocalcification by the marine alga *Emiliania huxleyi* (Lohmann) Hay and Mohler. Eur. J. Biochem. **99**, 559—567.

KLAVENESS, D., 1972 a: *Coccolithus huxleyi* (Lohmann) Kamptner. I. Morphological investigations on the vegetative cell and the process of coccolith formation. Protistologica **8**, 335—346.

— 1972 b: *Coccolithus huxleyi* (Lohmann) Kamptner. II. The flagellate cell, aberrant cell types, vegetative propagation and life cycles. Br. Phycol. J. **7**, 309—318.

PARKE, M., GREEN, J., 1976: Check-list of British marine algae—third revision. J. mar. biol. Ass. U.K. **56**, 527—594.

SHAW, F. D., MORRIS, J. F., 1980: Calcium localization in the rat neurohypophysis. Nature **287**, 56—58.

SIKES, C. S., ROER, R. D., WILBUR, K. M., 1980: Photosynthesis and coccolith formation: Inorganic carbon sources and net inorganic reaction of deposition. Limnol. Oceanogr. **25**, 248—261.

TAPPAN, H., 1980: The paleobiology of plant protists. San Francisco: Freeman.

WAL, P. VAN DER, JONG, E. W. DE, WESTBROEK, P., and BRUIJN, W. C. DE, 1983 a: Calcification in the coccolithophorid alga *Hymenomonas carterae*. Ecol. Bull. **35**, 251—258.

— — — — MULDER-STAPEL, A. A., 1983 b: Ultrastructural polysaccharide localization in calcifying and naked cells of the coccolithophorid *Emiliania huxleyi*. Protoplasma **118**, 157—168.

WATABE, N., WILBUR, K. M., 1976: The mechanisms of mineralization in the invertebrates and plants. University of South Carolina Press, Columbia, S.C., XII + 461 p.

WICK, S. M., HEPLER, P. K., 1982: Selective localization of intracellular Ca^{2+} with potassium antimonate. J. Histochem. Cytochem. **30**, 1190—1204.

WILBUR, K. M., WATABE, N., 1963: Experimental studies in calcification in molluscs and the alga *Coccolithus huxleyi*. Ann. N.Y. Acad. Sci. **109**, 82—112.